Inertial mass sensing with low Q-factor vibrating microcantilevers

S. Adhikari
Zienkiewicz Centre for Computational Engineering, Swansea University, Bay Campus, Swansea SA1 8EN, United Kingdom

(Received 30 June 2017; accepted 23 September 2017; published online 12 October 2017)

Mass sensing using micromechanical cantilever oscillators has been established as a promising approach. The scientific principle underpinning this technique is the shift in the resonance frequency caused by the additional mass in the dynamic system. This approach relies on the fact that the Q-factor of the underlying oscillator is high enough so that it does not significantly affect the resonance frequencies. We consider the case when the Q-factor is low to the extent that the effect of damping is prominent. It is shown that the mass sensing can be achieved using a shift in the damping factor. We prove that the shift in the damping factor is of the same order as that of the resonance frequency. Based on this crucial observation, three new approaches have been proposed, namely, (a) mass sensing using frequency shifts in the complex plane, (b) mass sensing from damped free vibration response in the time domain, and (c) mass sensing from the steady-state response in the frequency domain. Explicit closed-form expressions relating absorbed mass with changes in the measured dynamic properties have been derived. The rationale behind each new method has been explained using non-dimensional graphical illustrations. The new mass sensing approaches using damped dynamic characteristics can expand the current horizon of micromechanical sensing by incorporating a wide range of additional measurements. *Published by AIP Publishing.* https://doi.org/10.1063/1.4993678

I. INTRODUCTION

Label-free mass sensing using cantilever-like resonators is an active field of multidisciplinary research.[1,2] Depending on the size on the cantilever, the mass to be detected can vary from few atoms to relatively larger size like DNA and other biological molecules.[3–8] With the advancement of manufacturing technology, micrometer size cantilever sensors are expected to be used in practice in the near future for a variety of applications including biosensors, environmental sensor, gas sensors, and chemical sensors.[6,9–14]

For any mechanical sensors to work in a reliable manner, it is necessary that the object to be sensed makes a detectable change in a quantity which can be measured easily and accurately. The measurement of the resonance frequency is one of the most fundamental properties of an oscillator and can be measured reliably across a wide range of mechanical systems. Resonance based sensors offer significant potential of achieving the high-fidelity requirement of many sensing applications.[15–27] The central principle of mass detection is based on the fact that the effective resonance frequency of the oscillator is reduced when additional mass is attached. Using the reduction of the natural frequency, commonly termed as the frequency-shift, it is possible to "predict" how much mass is responsible for causing that change. The idea is in principle simple; however, there are a number of practical issues which can influence the mass detection significantly. These include, but are not limited to, (1) the object absorbed on the cantilever is not a "point-mass" but has a finite dimension, (2) the object has an intrinsic stiffness such that it can alter the effective stiffness of the underlying cantilever and therefore change the frequency in a different manner, (3) the position of the object absorbed on the cantilever may not be precisely known, (4) the "attachment" between the object and the cantilever may not be perfectly rigid, (5) the shape of the object can introduce other mechanical effects such as rotary inertia and shear deformation, (6) the chemical composition and/or the surface tension of the object can introduce local surface stress to an extent that it alters the dynamics of the cantilever, and (7) the attached object itself can vibrate and therefore may bring new dynamics to the system. These issues, among many other issues, are still active areas of investigations (see, for example, Refs. 28–31).

Dynamic characteristics of resonators used for mass sensing is crucially affected by their Q-factors or damping factors.[32–36] In general, the higher the Q-factor, the better the quality of the measurement of the resonance frequencies. This is because (a) high Q-factor leads to a sharper peak in the frequency response making it easy to identify the resonance frequency, and (b) signal to noise ratio becomes much high when the Q-factor is high. Therefore, a broad aim of most sensor design is to have as high Q-factor as possible. While recent studies have shown that it is possible to have oscillators to have very high Q-factors, in some cases this may not be always possible. One example is cantilever sensors immersed in a fluidic environment[37,38] where the surrounding fluid can be a source of viscous damping. For linear systems, the effect of damping is most pronounced in the dynamic response near the resonance frequency in the frequency response function. We refer to these books[39–42] for further discussions on general analysis and modelling of damping in dynamic systems. Unlike the inertia and stiffness forces, the theoretical modelling of damping from the first principles is not a general approach. Normally this is done in

a case by case basis by investigating damping mechanisms of a particular dynamic problem. For simplification, it is customary to model damping by a viscous damping factor, which presents an equivalent damping of the system. The effect of the damping factor on the resonance frequency is small. For this reason, micromechanical mass sensing methods derived based on the assumption of undamped system dynamics, as normally done in practice, is valid for lightly damped systems also. This aspect will be investigated further in this paper.

Micromechanical mass sensing based on resonance frequency shift approach relies on the fact the inherent damping in the system is small (high Q-factor). The aim of this work is to relax this assumption and consider cantilever resonators with high damping. It will be shown that in this situation, mass sensing methods alternative to measuring the resonance frequency is possible. Consequently, the frequency-shift is not the only measurement that needs to be employed for mass sensing. The outline of the paper is as follows: In Sec. II, the equation of motion of damped cantilevers is discussed. In particular, in Subsection II A, the continuum model is shown, and the corresponding single degree of freedom approximation is obtained in Subsection II B. Dynamic analysis of mass absorbed damped cantilevers is discussed in Sec. III, and the key results necessary for mass sensing is derived. The main techniques for mass sensing exploiting the damped dynamics are developed in Sec. IV. Three main ideas have been put forward, namely, (1) mass sensing using frequency shifts in the complex plane (in Subsection IV A), (2) mass sensing from damped free vibration response in the time domain (in Subsection IV B), and (3) mass sensing from the steady-state response in the frequency domain (in Subsection IV C). Finally, Sec. V summarises the work and draws some conclusions.

II. EQUATION OF MOTION OF DAMPED CANTILEVERS

A. The exact partial differential equation

The dimension of microcantilevers can vary depending on applications. Typically, the dimensions are in the order of 100 μm long, 50 μm wide, and 0.5 μm thick.[1] Due to the small thickness to length ratio, Euler-Bernoulli beam theory can be used to model bending vibration of such microcantilevers. The equation of motion of a damped cantilever modelled (see, for example, Ref. 43) using Euler-Bernoulli beam theory can be expressed as

$$EI\frac{\partial^4 U(x,t)}{\partial x^2}+\hat{c}_1\frac{\partial^5 U(x,t)}{\partial x^4\partial t}+\rho A\frac{\partial^2 U(x,t)}{\partial t^2}+\hat{c}_2\frac{\partial U(x,t)}{\partial t}=F(x,t). \tag{1}$$

In the above equation, x is the coordinate along the length of the beam, t is the time, E is the Young's modulus, I is the second-moment of the cross-section, A is the cross-section area, ρ is the density of the material, $F(x, t)$ is the applied spatial dynamic forcing, and $U(x, t)$ is the transverse displacement. The length of the beam is assumed to be L. Additionally $\hat{c}_1$ is the strain-rate-dependent viscous damping coefficient, and $\hat{c}_2$ is the velocity-dependent viscous damping coefficient. The strain-rate-dependent damping can be used to model inherent damping property of the material of the cantilever beam. The velocity-dependent viscous damping can be used to model damping due to external factors such as a cantilever immersed in a fluidic environment. A schematic diagram of a cantilever micromechanical sensor immersed in a viscous fluid is shown in Fig. 1. The viscous fluid is used for illustration purpose only. Its main role for the purpose of this paper is that it simulates external damping to the vibrating system. We refer to other works[37,38] for more detailed discussions on vibrating cantilevers in fluid. The undamped natural frequencies (Hz) of a cantilever resonator can be expressed as

$$f_j=\frac{\lambda_j^2}{2\pi}\sqrt{\frac{EI}{\rho AL^4}},\quad j=1,2,3,\ldots \tag{2}$$

where λ_j needs to be obtained by[44] solving the following transcendental equation:

$$\cos\lambda\cosh\lambda+1=0. \tag{3}$$

Solving this equation, the values of λ_j can be obtained as 1.8751, 4.69409, 7.8539 and 10.99557. For larger values of j, in general, we have $\lambda_j=(2j-1)/2\pi$. The vibration mode shape corresponding to the j-th natural frequency can be expressed as

$$\phi_j(\xi)=\left(\cosh\lambda_j\xi-\cos\lambda_j\xi\right)-\left(\frac{\sinh\lambda_j-\sin\lambda_j}{\cosh\lambda_j+\cos\lambda_j}\right)\times\left(\sinh\lambda_j\xi-\sin\lambda_j\xi\right), \tag{4}$$

where $\xi=\frac{x}{L}$ is the normalised coordinate along the length of the cantilever. For sensing applications, we are primarily interested in the first few modes of vibration only.

Consider the attached object of mass M at the end of the cantilevered resonator in Fig. 1. The boundary conditions with an additional mass of M at $x=L$ can be expressed as

$$U(0,t)=0,\quad U'(0,t)=0,\quad U''(L,t)=0,\quad \text{and}\quad EIU'''(L,t)-M\ddot{U}(L,t)=0. \tag{5}$$

Here, $(\bullet)'$ denotes derivative with respective to x and $(\dot{\bullet})$ denotes derivative with respective to t. It can be shown that

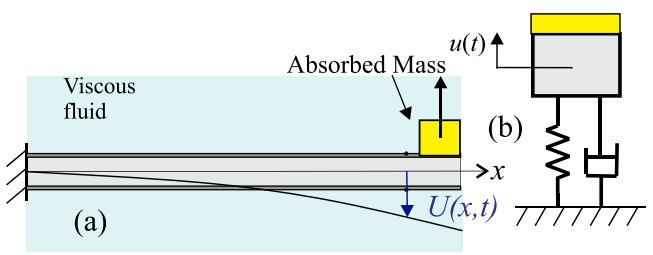

FIG. 1. Schematic diagrams of: (a) a cantilever micromechanical mass sensor immersed in a viscous fluid, and (b) an equivalent damped single degree of freedom model oscillator model.

(see, for example, Ref. 28) the resonance frequencies are still obtained from Eq. (2) but λ_j should be obtained by solving

$$(\cos\lambda\sinh\lambda-\sin\lambda\cosh\lambda)\Delta M\,\lambda+(\cos\lambda\cosh\lambda+1)=0. \tag{6}$$

Here

$$\Delta M=\frac{M}{\rho AL} \tag{7}$$

is the ratio of the added mass and the mass of the cantilever. If the added mass is zero, then one can see that Eq. (7) reduces to Eq. (3). For this general case, the eigenvalues λ_j as well as the mode shapes $\phi_j(\xi)$ become a function of ΔM. Unlike the classical mass-free case, closed-from expressions are not available. However, very accurate approximation can be developed for this case.[28]

B. Equivalent single degree of freedom model

The equation of motion of the beam in (1) is a partial differential equation. This equation represents infinite number of degrees of freedom. The mathematical theory of linear partial differential equations is very well developed and the nature of solutions of the bending vibration is well understood. Considering the steady-state harmonic motion with frequency ω we have

$$U(x,t)=u(x)\exp[\mathrm{i}\omega t], \tag{8}$$

$$\text{and}\quad F(x,t)=f(x)\exp[\mathrm{i}\omega t], \tag{9}$$

where $\mathrm{i}=\sqrt{-1}$. Substituting this in the beam equation (1) we have

$$EI\frac{d^4u(x)}{dx^4}+\mathrm{i}\omega\hat{c}_1\frac{d^4u(x)}{dx^4}-\rho A\omega^2u(x)+\mathrm{i}\omega\hat{c}_2u(x)=f(x). \tag{10}$$

Following the damping convention in dynamic analysis as in Ref. 45, we consider stiffness and mass proportional damping. Therefore, we express the damping constants as

$$\hat{c}_1=\alpha(EI)\quad\text{and}\quad\hat{c}_2=\beta(\rho A), \tag{11}$$

where α and β are stiffness and mass proportional damping factors. Substituting these, from Eq. (10), we have

$$EI\frac{d^4u(x)}{dx^4}+\mathrm{i}\omega\underbrace{\left(\alpha EI\frac{d^4u(x)}{dx^4}+\beta\rho Au(x)\right)}_{\text{damping}}-\rho A\omega^2u(x)=f(x). \tag{12}$$

The first part of the damping expression is proportional to the stiffness term while the second part of the damping expression is proportional the mass term. The general solution of Eq. (12) can be expressed as a linear superposition of all the vibration mode shapes (see, for example, Ref. 45). Micromechanical mass sensors are often designed to operate within a frequency range which is close to fist few natural frequencies only. Therefore, without any loss of accuracy, simplified lumped parameter models can be used to corresponding correct resonant behaviour. This can be achieved using energy methods or more generally using Galerkin approach.

Galerkin approach can be employed in the time domain or in the frequency domain. We adopt a time domain approach. The necessary changes to apply this in the frequency domain are straightforward for linear problems and therefore not elaborated here. Assuming a unimodal solution, the dynamic response of the beam can be expressed as

$$U(x,t)=u_j(t)\phi_j(x),\quad j=1,2,3,\ldots. \tag{13}$$

Substituting this assumed motion into the equation of motion (1), multiplying by $\phi_j(x)$ and integrating by parts over the length one has

$$\begin{aligned}&EIu_j(t)\int_0^L\phi_j''^2(x)\mathrm{d}x+\alpha EI\dot{u}_j(t)\int_0^L\phi_j''^2(x)\mathrm{d}x\\&+\beta\rho A\dot{u}_j(t)\int_0^L\phi_j^2(x)\mathrm{d}x+\rho A\ddot{u}_j(t)\int_0^L\phi_j^2(x)\mathrm{d}x\\&=\int_0^L F(x,t)\phi_j(x)\mathrm{d}x.\end{aligned} \tag{14}$$

Using the equivalent mass, damping, and stiffness, this equation can be rewritten as

$$m_{eq_j}\ddot{u}_j(t)+c_{eq_j}\dot{u}_j(t)+k_{eq_j}u_j(t)=f_j(t), \tag{15}$$

where the equivalent mass and stiffness terms are given by

$$m_{eq_j}=\rho A\int_0^L\phi_j^2(x)\mathrm{d}x=\rho AL\underbrace{\int_0^1\phi_j^2(\xi)\mathrm{d}\xi}_{I_{1_j}}, \tag{16}$$

$$k_{eq_j}=EI\int_0^L\phi_j''^2(x)\mathrm{d}x=\frac{EI}{L^3}\underbrace{\int_0^1\phi_j''^2(\xi)\mathrm{d}\xi}_{I_{2_j}}. \tag{17}$$

The equivalent damping and the equivalent forcing are expressed as

$$c_{eq_j}=\alpha k_{eq_j}+\beta m_{eq_j}, \tag{18}$$

$$f_j(t)=\int_0^L F(x,t)\phi_j(x)\mathrm{d}x. \tag{19}$$

Using the expression of the mode-shape in Eq. (4), the integrals I_{1_j} and I_{2_j} can be evaluated in closed-form for any general mode as

$$\begin{aligned}I_{1_j}=&(-\cos\lambda_j\sinh\lambda_j-\cos^2\lambda_j\cosh\lambda_j\sinh\lambda_j\\&+\lambda_j\cos^2\lambda_j-\cosh\lambda_j\sin\lambda_j-\cos\lambda_j\cosh^2\lambda_j\sin\lambda_j\\&+2\cos\lambda_j\cosh\lambda_j\lambda_j+\lambda_j\cosh^2\lambda_j)/\left(D\lambda_j\right),\end{aligned} \tag{20}$$

$$\begin{aligned}I_{2_j}=&\lambda_j^3(3\cos\lambda_j\sinh\lambda_j+3\cos^2\lambda_j\cosh\lambda_j\sinh\lambda_j\\&+\lambda_j\cos^2\lambda_j+3\cosh\lambda_j\sin\lambda_j+\lambda_j\cosh^2\lambda_j\\&+3\cos\lambda_j\cosh^2\lambda_j\sin\lambda_j+2\cos\lambda_j\cosh\lambda_j\lambda_j)/D.\end{aligned} \tag{21}$$

The denominator D is given by

$$D = \cosh^2\lambda_j + 2\cos\lambda_j\cosh\lambda_j + \cos^2\lambda_j. \tag{22}$$

For the first mode of vibration ($j=1$), substituting $\lambda_1 = 1.8751$, it can be shown that $I_{1_1} = 1$ and $I_{1_2} = 12.3624$. If there is a point mass of M at the tip of the cantilever, then the effective mass becomes

$$m_{eq_j} = \rho AL I_{1_j} + M\underbrace{\phi_j^2(1)}_{I_{3_j}} = \rho AL\left(I_{1_j} + \Delta M I_{3_j}\right). \tag{23}$$

Using the expression of the mode-shape, we have

$$I_{3_j} = \frac{4\sinh^2\lambda_j \sin^2\lambda_j}{D}. \tag{24}$$

For the first mode of vibration, it can be shown that $I_{3_1} = 4$. The equivalent single degree of freedom model given by Eq. (15) is used in the rest of the paper. However, the expression derived here is general and can be used if higher modes of vibration[46] were to be employed in sensing.

III. DYNAMIC CHARACTERISTICS OF MASS ABSORBED DAMPED OSCILLATORS

For notational simplification, from (15), the equation of motion of the equivalent single degree of freedom cantilever resonator without any added mass is expressed as

$$m_0\ddot{u}_0(t) + c_0\dot{u}_0(t) + k_0u_0(t) = f(t), \tag{25}$$

where

$$c_0 = \alpha k_0 + \beta m_0. \tag{26}$$

We call the oscillator given by Eq. (25) as the reference oscillator. Diving by m_0, the equation of motion can be expressed as

$$\ddot{u}_0(t) + 2\zeta_0\omega_0\dot{u}_0(t) + \omega_0^2u_0(t) = \frac{f(t)}{m_0}. \tag{27}$$

Here, the undamped natural frequency (ω_0) and the damping factor (ζ_0) are expressed as

$$\omega_0 = \sqrt{\frac{k_0}{m_0}}, \tag{28}$$

$$\text{and} \quad \frac{c_0}{m_0} = 2\zeta_0\omega_0 \quad \text{or} \quad \zeta_0 = \frac{c_0}{2\sqrt{k_0m_0}}. \tag{29}$$

In view of the expression of c_0 in (26), the damping factor can also be expressed in terms of the stiffness and mass proportional damping constants as

$$\zeta_0 = \frac{1}{2}\left(\alpha\omega_0 + \frac{\beta}{\omega_0}\right). \tag{30}$$

Taking the Laplace transform of Eq. (27), we have

$$s^2U_0(s) + s2\zeta_0\omega_0U_0(s) + \omega_0^2U_0(s) = \frac{F(s)}{m_0}, \tag{31}$$

where $U_0(s)$ and $F(s)$ are the Laplace transforms of $u_0(t)$ and $f(t)$, respectively. Solving the equation associated with coefficient of $U_0(s)$ in Eq. (27) without the forcing term, the complex natural frequencies of the system are given by

$$s_{0_{1,2}} = -\zeta_0\omega_0 \pm \mathrm{i}\omega_0\sqrt{1-\zeta_0^2} = -\zeta_0\omega_0 \pm \mathrm{i}\omega_{d_0}. \tag{32}$$

Here, the imaginary number $\mathrm{i} = \sqrt{-1}$ and the damped natural frequency is expressed as

$$\omega_{d_0} = \omega_0\sqrt{1-\zeta_0^2}. \tag{33}$$

For a damped oscillator, at resonance, the frequency of oscillation is given by $\omega_{d_0} < \omega_0$. Therefore, for positive damping, the resonance frequency of a damped system is always lower than the corresponding underlying undamped system.

The Quality factor (Q-factor) of an oscillator is the ratio between the energy stored and energy lost during one cycle when the oscillator vibrates at the resonance frequency. It can be shown that (omitting the subscript 0) the Q-factor

$$Q = \frac{m\omega_d}{c} = \frac{\sqrt{1-\zeta^2}}{2\zeta}. \tag{34}$$

Alternatively, the damping factor can be related to the Q-factor as

$$\zeta = \frac{1}{\sqrt{1+4Q^2}}. \tag{35}$$

We will use both factors as appropriate.

Let us now consider that due to the added mass, the new mass is given by

$$m_0 + m_0\Delta = m_0(1+\Delta). \tag{36}$$

The non-dimensional mass factor Δ quantifies the additional "absorbed mass." This is the primary quantity of interest which we want to identify by exploiting the dynamic behaviours of the damped oscillator. From a practical standpoint, $0 < \Delta \ll 1$. The equation of motion of the mass-absorbed oscillator is given by

$$m_0(1+\Delta)\ddot{u}_m(t) + c_0\dot{u}_m(t) + k_0u_m(t) = f(t). \tag{37}$$

Here, $u_m(t)$ is the displacement variable of the new system. Dividing by m_0 and taking the Laplace transform, we have

$$\left(s^2(1+\Delta) + s2\zeta_0\omega_0 + \omega_0^2\right)U_m(s) = \frac{F(s)}{m_0}. \tag{38}$$

Here, $U_m(s)$ is the Laplace transform of $u_m(t)$. It is assumed that *only* the mass of the system has changed. The damping and the stiffness of the system remain identical to the reference system. In this way we can precisely quantify the impact of the added mass on the dynamics of the system. The complex natural frequencies of the mass-absorbed oscillator are given by

$$s_{m_{1,2}} = -\frac{\zeta_0\omega_0}{(1+\Delta)} \pm \mathrm{i}\frac{\omega_0\sqrt{(1+\Delta)-\zeta_0^2}}{(1+\Delta)}. \tag{39}$$

Expressing $(1+\Delta) = \left(\sqrt{1+\Delta}\right)\left(\sqrt{1+\Delta}\right)$, this equation can be rewritten as

$$s_{m_{1,2}} = -\frac{\zeta_0}{\sqrt{1+\Delta}}\frac{\omega_0}{\sqrt{1+\Delta}} \pm \mathrm{i}\frac{\omega_0}{\sqrt{1+\Delta}}\sqrt{1-\left(\frac{\zeta_0}{\sqrt{1+\Delta}}\right)^2}. \tag{40}$$

We define the natural frequency and damping factor of the mass-absorbed oscillator as

$$\omega_m = \frac{\omega_0}{\sqrt{1+\Delta}}, \tag{41}$$

$$\text{and} \quad \zeta_m = \frac{\zeta_0}{\sqrt{1+\Delta}}. \tag{42}$$

Using these, from (40), the complex natural frequencies of the system can be given similar to Eq. (32) as

$$s_{m_{1,2}} = -\zeta_m\omega_m \pm \mathrm{i}\omega_m\sqrt{1-\zeta_m^2} = -\zeta_m\omega_m \pm \mathrm{i}\omega_{d_m}, \tag{43}$$

where the damped natural frequency of the mass-absorbed oscillator is expressed as

$$\omega_{d_m} = \omega_m\sqrt{1-\zeta_m^2} = \frac{\omega_0\sqrt{(1+\Delta)-\zeta_0^2}}{(1+\Delta)}. \tag{44}$$

After some algebra, this can be related to the damped natural frequency of the reference system as

$$\omega_{d_m} = \frac{\omega_{d_0}}{\sqrt{1+\Delta}}\sqrt{\frac{1-\zeta_0^2/(1+\Delta)}{1-\zeta_0^2}}. \tag{45}$$

Using Eqs. (34), (35), and (42), the Q-factor of the mass-absorbed oscillator can be related to the reference oscillator as

$$Q_m = \sqrt{Q_0^2(1+\Delta)+\frac{\Delta}{4}}. \tag{46}$$

Equations (41), (42), (45), and (46) completely relate the undamped natural frequency, damping factor, damped natural frequency, and Q-factor of the mass-absorbed oscillator to that of the reference oscillator. The conventional assumptions small damping (large Q-factor) and small mass change have not been used in these derivations. For oscillators with small damping, that is, $\zeta_0 \ll 1$, Eqs. (45) and (46) can be approximated as

$$\omega_{d_m} \approx \frac{\omega_{d_0}}{\sqrt{1+\Delta}}, \tag{47}$$

$$\text{and} \quad Q_m \approx Q_0\sqrt{1+\Delta}. \tag{48}$$

Based on this analysis, the following important points can be established:

1. The undamped natural frequency of the mass-absorbed oscillator is less than that of the reference oscillator. The difference in the value of the frequency, or the "frequency shift" as commonly referred to, can be quantified by Eq. (41).
2. The damping factor of the mass-absorbed oscillator is less than that of the reference oscillator and can be quantified by Eq. (42). The amount of change in the damping factor is *exactly* the same as the change in the undamped natural frequency.
3. Following on from the above observation, the Q-factor of the mass-absorbed oscillator is more than that of the reference oscillator and can be quantified by Eq. (46) or approximately by Eq. (48). If the approximation is considered, then the change in the Q-factor exactly reflects the change in the damping factor (that is, by $\sqrt{1+\Delta}$).
4. Similar to the undamped natural frequency, the damped natural frequency of the mass-absorbed oscillator is less than that of the reference oscillator. The frequency shift can be quantified by Eq. (45) or approximately by Eq. (47). If the approximation is considered, then the frequency shift of the undamped and damped natural frequencies becomes the same.

The first observation regarding the shift in the undamped natural frequency is very well known. In fact, this is the primary scientific basis behind micromechanical mass sensing. However, observations 2 and 3 above show that the added mass changes the damping factor and the Q-factor by a similar amount. This fact has not been exploited in micromechanical mass sensing. Just like what is done with the undamped frequency shift, any experimental technique to measure the damping factor or the Q-factor can be used for mass sensing. This can be employed when the conventional frequency shift analysis becomes difficult to apply accurately, for example, in a low Q-system. Alternatively, mass sensing from the damping factor and Q-factor shift can be used in conjunction with the classical frequency shift analysis. Results using this new approach can either be used to validate frequency shift based results or can be averaged to obtain more robust and consistent results. It should be emphasised that the high Q-factor assumption only simplifies certain mathematical expressions. This assumption is *not* necessary to establish the fundamental fact behind the damping factor and Q-factor shift. For high Q-factor oscillators, from Eqs. (41), (42), (48), and (47), we observe that the undamped natural frequency changes by exactly the same amount as the damping factor, Q-factor, and the damped natural frequency.

It is important to physically understand the reasons behind these observations so that they are not just artefacts arising from mathematical manipulations in Eq. (40). When an additional mass is added to an existing oscillator, it becomes heavier. As a result, the "new" oscillator vibrates slowly and therefore results in a natural frequency which is lower than the reference natural frequency. This is what has been quantified in Eq. (41) for the undamped natural frequency and in Eq. (45) for the damped natural frequency. When the free vibration at resonance is considered, the

oscillator with an additional mass has more kinetic energy compared to the reference oscillator. As the stiffness and damping remain the same, this additional energy allows the oscillator to vibrate for longer (although at a slower frequency). This is reflected by a lower effective damping factor as given by Eq. (42). Alternatively, if the peak response at the resonance frequency is considered, the extra kinetic energy would result in a higher vibrational amplitude. This, in turn, would be reflected by a higher and sharper peak at the resonance, resulting in an effective increase of the Q-factor as quantified in (46). In Sec. IV, we explore some ideas on how to exploit the changes in these fundamental dynamic properties of an oscillator for inertial mass sensing.

IV. APPROACHES TO MASS SENSING USING DAMPED DYNAMICS

In Sec. III, we have pointed out that the changes in the damping factor and the Q-factor due to an added mass to a damped oscillator can provide an alternative route to micromechanical mass sensing. This can be used in conjunction with the conventional frequency shift based approaches or can be established as a new avenue. In Secs. IV A–IV C, three distinct approaches are suggested based on the nature of experimental measurements. These include (1) frequency shifts in the complex plane, (2) free vibration response in the time domain, and (3) steady-state response in the frequency domain.

A. Mass sensing using frequency shifts in the complex plane

The complex frequency in given by Eq. (43) has the real and imaginary parts as follows:

$$\Re(s_m) = -\zeta_m \omega_m = -\frac{\zeta_0 \omega_0}{(1+\Delta)}, \tag{49}$$

$$\text{and} \quad \Im(s_m) = \omega_{d_m} = \frac{\omega_0 \sqrt{(1+\Delta) - \zeta_0^2}}{(1+\Delta)}. \tag{50}$$

The real part is always negative for a stable system and it is related to the decay rate of the dynamic response. The imaginary part corresponds to the oscillation frequency of the dynamic response of the damped system. In Fig. 2, these quantities are plotted for five different values of the Q-factors of the reference oscillator. The value of the added mass is considered up to $\Delta = 0.5$ for illustrative purposes. From this plot, the following observation can be made:

1. When the Q-factor of the reference oscillator is very high, as can be seen in lines for $Q_0 = 250$ in Fig. 2, the effect of added mass is only pronounce in the oscillation frequency. Its effect on the decay rate is negligible when viewed in this scale. This is the primary reason why most micromechanical sensing approach exploits the frequency shift only (changes in the Y-axis in Fig. 2).
2. The Q-factor of the reference oscillator does not have a significant effect on the change in the oscillation frequency due to the added mass. This can be seen from Fig. 2 that the change in the Y-axis is confined within 1–0.8 (0.8165 to be precise) for a change of mass $\Delta = 0.5$.
3. When the Q-factor of the reference oscillator is low (less than 50), noticeable change in the real part of the complex frequency can be observed. Unlike the imaginary part where the total change in independent of the Q-factor, the total change in the real part increases with lower Q-factor. Therefore, it is clear that in a low Q-factor situation, the changes in the decay rate of the oscillator can be a credible pathway for inertial mass sensing.

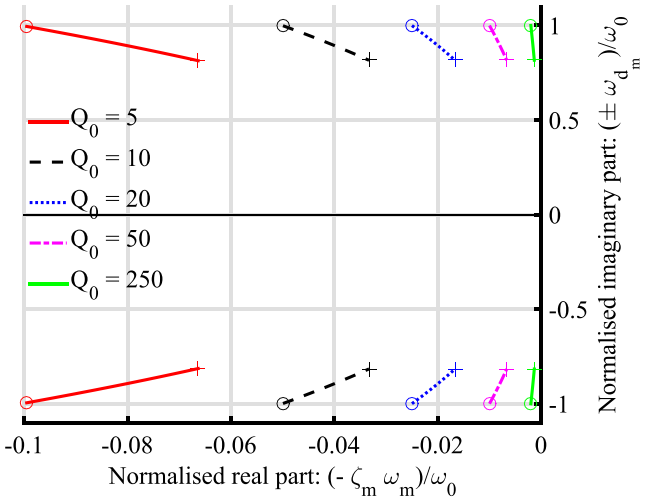

FIG. 2. The variation of the complex frequency in (43) (normalised by ω_0) due to the added mass on the oscillator with different Q-factors. The point "o" indicates the frequency for the reference oscillator and the point "+" denotes the frequency when the added mass factor $\Delta = 0.5$. The X-axis corresponds to the decay rate while the Y-axis corresponds to the oscillation frequency of the dynamic response.

In Fig. 3, the absolute change in the real and imaginary parts of the complex frequency due to the addition of mass is

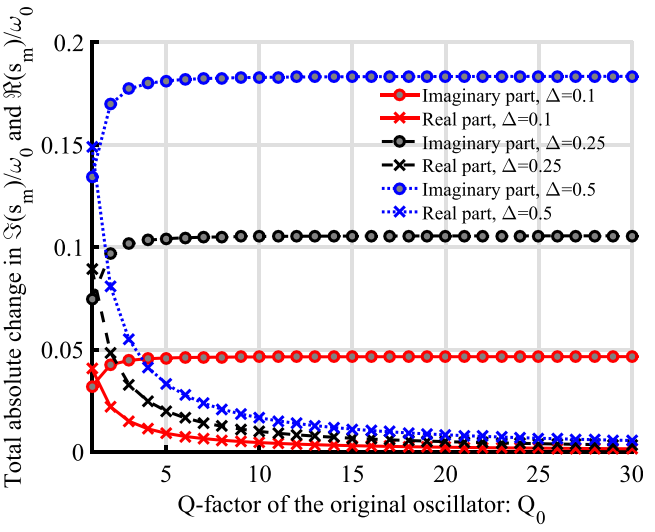

FIG. 3. The absolute change in the real and imaginary parts of the complex frequency (normalised by ω_0) due to the addition of mass as a function of the Q-factor of the reference oscillator.

shown. The changes are normalised by ω_0 and the results are plotted as a function of the Q-factor of the reference oscillator. Except for very low Q, the absolute change in the imaginary part is always higher than that of the real part when viewed together in one plot (note that the physical meanings of the real and imaginary parts are very different). Additionally, the nature of the change in the real and imaginary parts is drastically different. The changes in the imaginary part (oscillation frequency) is independent of the Q-factor when $Q_0 > 5$. It also remains distinctly different for different values of the added mass Δ. On the other hand, the absolute change in the real part reduces with increasing Q-factor. For oscillators with larger Q-factors, the absolute change in the real part becomes very small and effectively indistinguishable for different values Δ. Figure 3 illustrates clearly why the change in the imaginary part is the most appealing quantify for mass sensing.

Although the complex frequency appears as a single quantity in (43), the measurement of the real and imaginary parts, in general, requires quite different approaches. The real part (decay rate) is easier to measure in low-Q systems, while the imaginary part (oscillation frequency) is easier to measure in high-Q systems with sharper response peaks. Experimental techniques are constantly improving and it is reasonable to assume that both the real and imaginary parts can be accurately measured for a wide range of micromechanical systems. The consideration of complex frequency offers a mathematically richer potential for micromechanical inertial sensing compared to the only oscillation frequency based approach which restricts the problem on the imaginary axis only. Since we established in Fig. 3 that the changes in the real part alone is unlikely to offer a realistic prospect, we investigate the two other cases, namely, (a) the consideration of the complex frequency, and (b) the consideration of only the imaginary part of the complex frequency (the classical case).

1. The consideration of the complex frequency

It is assumed that the complex frequency (that is, both the real and imaginary parts) of the reference oscillator is known. Once the oscillator is mass-absorbed, the complex frequency is experimentally measured again. A key aim of micromechanical sensing is to be able to detect the mass from the change in the frequency. With two complex numbers, the change can be established either by the calculating the absolute of the difference or by difference of the absolutes. We adopt the second quantity as it turns out to give simpler analytical expressions for the absorbed mass. We define the normalised complex frequency shift parameter as

$$\begin{aligned}\Delta\hat{f}^2 &= \frac{1}{\omega_0^2}\left(|s_0|^2 - |s_m|^2\right)\\ &= \frac{1}{\omega_0^2}\left[\left\{\left(\Re(s_0)\right)^2 - \left(\Re(s_m)\right)^2\right\}\right.\\ &\quad \left.+\left\{\left(\Im(s_0)\right)^2 - \left(\Im(s_m)\right)^2\right\}\right]. \end{aligned} \tag{51}$$

We use the notation $\Delta\hat{f}$ which is normally used when the frequency is given in Hz. However, as we consider a normalisation with respect to ω^2, the unit of the frequency (Hz or rad/s) does not change the value of $\Delta\hat{f}$. Using the expressions in Eqs. (49) and (50), the above equation can be simplified to

$$\begin{aligned}\Delta\hat{f}^2 &= \left\{\zeta_0^2 - \frac{\zeta_0^2}{(1+\Delta)^2}\right\} + \left\{1 - \zeta_0^2 - \frac{1+\Delta-\zeta_0^2}{(1+\Delta)^2}\right\}\\ &= \frac{\Delta}{1+\Delta}. \end{aligned} \tag{52}$$

From the normalised complex frequency shift, the absorbed mass can be obtained as

$$\Delta = \frac{1}{1-\Delta\hat{f}^2} - 1. \tag{53}$$

A rather unexpected observation from this equation is that the absorbed mass is independent of the Q-factor of the reference oscillator. This implies that if (measured) complex frequencies are used, the mass identification equation (53) can be used for any oscillator irrespective of their Q-factor.

2. The consideration of only the imaginary part of the complex frequency

The mass identification equation in (53) appears to be similar to the classical case[18,28] when only the undamped oscillation frequency is used (that is only the real part and ignoring the damping). The key difference between (53) and similar equations obtained only from the consideration of the resonance frequency shift is that the real part of the complex frequency is ignored in the calculations. As this is a common practice, we investigate this case when the Q-factor of the reference oscillator is low. For damped systems, any experimental measurement always measures the damped frequency. This is because at resonance the cantilever sensor oscillates with the damped frequency (ω_d) and *not* with the undamped frequency. Therefore, we define the normalised damped frequency shift as

$$\Delta\tilde{f} = \frac{1}{\omega_0}\left\{\Im(s_0) - \Im(s_m)\right\}. \tag{54}$$

Unlike the previous case in (51), this is defined by the difference in two frequencies and not by their squared values. Using the expressions in Eq. (50), the above equation can be simplified to

$$\Delta\tilde{f} = \sqrt{1-\zeta^2} - \frac{\sqrt{1+\Delta-\zeta^2}}{(1+\Delta)}. \tag{55}$$

After some algebraic manipulations, this can be expressed by a quadratic equation in Δ and its relevant root can be given by

$$\Delta = \frac{-2\Delta\tilde{f}^2 + 4\Delta\tilde{f}\sqrt{1-\zeta_0^2} - 1 + 2\zeta_0^2 + \sqrt{1 - 4\Delta\tilde{f}^2\zeta_0^2 + 8\Delta\tilde{f}\sqrt{1-\zeta_0^2}\zeta_0^2 - 4\zeta_0^2 + 4\zeta_0^4}}{2\left(-\Delta\tilde{f} + \sqrt{1-\zeta_0^2}\right)^2}. \tag{56}$$

This is the *exact* equation which gives the mass absorption factor Δ from the measured (normalised) frequency shift $\Delta\tilde{f}$ of a damped oscillator. If it is assumed that the Q-factor of the reference oscillator is high ($\zeta_0^2 \approx 0$), then the above equation simplifies to the well known special case as

$$\Delta \approx \frac{2\Delta\tilde{f} - (\Delta\tilde{f})^2}{\left(1-\Delta\tilde{f}\right)^2} = \frac{1}{\left(1-\Delta\tilde{f}\right)^2} - 1, \tag{57}$$

$$= 2(\Delta\tilde{f}) + 3(\Delta\tilde{f})^2 + 3(\Delta\tilde{f})^3 + \cdots. \tag{58}$$

The last equation is obtained by expanding the right hand side of Eq. (57) in a Taylor series about $\Delta\tilde{f} = 0$. Therefore, when the Q-factor is very high ($\zeta_0^2 \approx 0$) and the measured frequency shift is small compared to the frequency of the oscillator ($(\Delta\tilde{f})^n \approx 0, \forall n \geq 2$), the exact equation for mass identification in Eq. (56) reduces to $\Delta \approx 2(\Delta\tilde{f})$ by keeping the first term in the series in (58).

B. Mass sensing from damped free vibration response in the time domain

Free vibration response of a damped oscillator can be used to obtain the decay rate. The dynamic response of the mass-absorbed oscillator in (37) due to an initial displacement u_{i_0} and initial velocity $\dot{u}_{i_0}$ can be expressed following[47] as:

$$u_m(t) = A_m e^{-\zeta_m\omega_m} \sin\left(\omega_{d_m}t + \phi_m\right), \tag{59}$$

$$\text{where } A_m = \sqrt{\frac{\left(\dot{u}_{i_0} + \zeta_m\omega_m u_{i_0}\right)^2 + \left(\omega_{d_m}u_{i_0}\right)^2}{\omega_{d_m}^2}}, \tag{60}$$

$$\text{and} \quad \phi_m = \tan^{-1}\frac{\omega_{d_m}u_{i_0}}{\dot{u}_{i_0} + \zeta_m\omega_m u_{i_0}}. \tag{61}$$

In Fig. 4, the dynamic response given by Eq. (59) is used for zero initial velocity and is plotted by normalising it with u_{i_0}. The time axis is normalised with the undamped time period of the reference oscillator

$$T_0 = \frac{2\pi}{\omega_0}. \tag{62}$$

Observe that the mass-absorbed oscillator vibrates for longer period with higher amplitudes with lower frequency. These plots confirm that the mass-absorbed oscillator has a lower resonance frequency and damping factor as given by Eqs. (41) and (42). To investigate this further, we show a representative case in Fig. 5. The difference in the decay rate of the response of the reference oscillator and the mass-absorbed oscillator can be seen clearly. Therefore, by

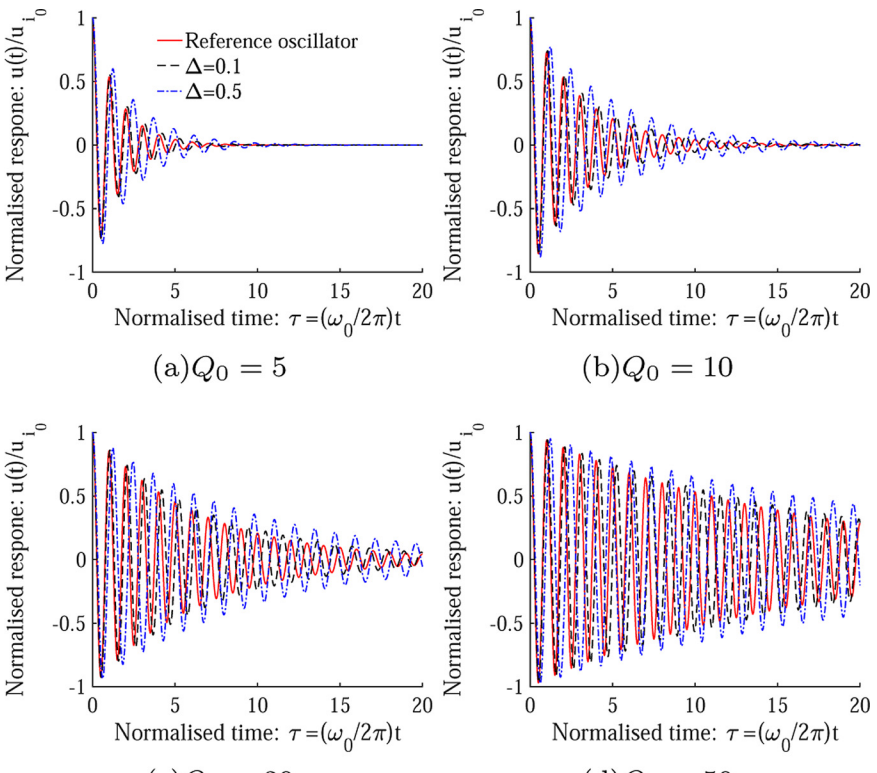

FIG. 4. Normalised response of the oscillator in the time domain due to an initial displacement plotted as a function of normalised time $\tau = t/T_0$ for two different mass absorption factors Δ and four different Q-factors.

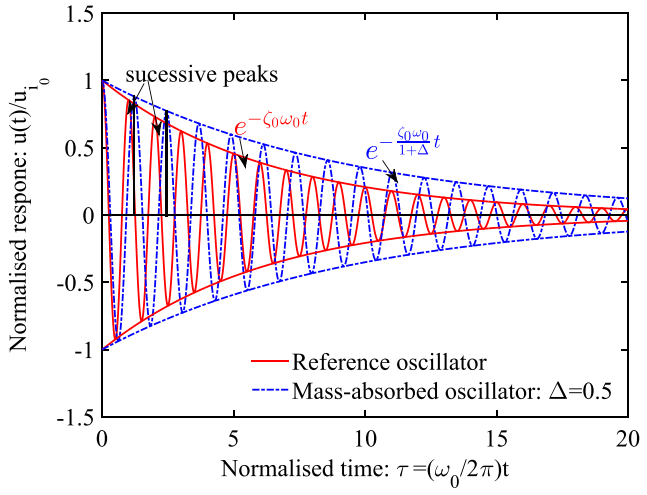

FIG. 5. Normalised response of the oscillator in the time domain due to an initial displacement plotted as a function of normalised time $\tau = t/T_0$ for mass absorption factor $\Delta = 0.5$ and $Q_0 = 20$.

measuring the decay rate, it would be possible to identify the mass absorption factor Δ from their difference. This can be done by directly measuring the displacement or velocity readouts (using optical readout for example) and obtaining two successive peaks as shown in Fig. 5.

Among various available techniques, the logarithmic decrement method (see for example Ref. 47) is one of the simplest and provides reasonably accurate results for the damping factors from the measured peaks. The main idea is to measure the height of two (or more) successive peaks and obtain the damping factor from the decrement. For any given damped oscillator, the *logarithmic decrement* is defined as

$$\delta = \ln \frac{u(t)}{u(t+T)}. \tag{63}$$

Using the expression of $u(t)$ as given in Eq. (59), it can be shown that for the mass-absorbed oscillator

$$\delta_m = \frac{2\pi\zeta_m}{\sqrt{1-\zeta_m^2}}. \tag{64}$$

In a similar way, the logarithmic decrement for the reference oscillator δ_0 can also be expressed. Assuming that the logarithmic decrements for the reference oscillator and the mass-absorbed oscillator have been experimentally measured from the response readouts, we propose an approach for obtaining the mass absorption factor.

Taking the ratio of the logarithmic decrements for both the oscillators we have

$$\frac{\delta_0}{\delta_m} = \frac{\zeta_0}{\zeta_m}\frac{\sqrt{1-\zeta_m^2}}{\sqrt{1-\zeta_0^2}}. \tag{65}$$

Using Eq. (42), and taking the square of the above equation one obtains

$$\left(\frac{\delta_0}{\delta_m}\right)^2 = \frac{1+\Delta-\zeta_0^2}{1-\zeta_0^2}. \tag{66}$$

The mass absorption factor therefore can be obtained by solving this equation as

$$\Delta = \left(1-\zeta_0^2\right)\left\{\left(\frac{\delta_0}{\delta_m}\right)^2 - 1\right\}. \tag{67}$$

Although this sensing technique relies on the measurement of the decrement of the dynamic response, small damping is not a requirement for this to be applicable. For systems with even very high Q-factor, the logarithmic decrements can be calculated by measuring response peaks several cycles apart as

$$\delta = \frac{1}{n}\ln\frac{u(t)}{u(t+nT)}. \tag{68}$$

Here, $n > 1$, is the number of periods the measured peaks are apart. When the Q-factor of the reference oscillator is high ($\zeta_0^2 \approx 0$), Eq. (67) can be further simplified as

$$\Delta \approx \left(\frac{\delta_0}{\delta_m}\right)^2 - 1. \tag{69}$$

Having established that the response decrement can be used for mass sensing in addition to the conventional frequency shift approach, in Sec. IV C we investigate methods in the frequency domain.

C. Mass sensing from the steady-state response in the frequency domain

The mass sensing approach developed in Sec. IV B is based on the transient response due to initial conditions. In many situations the cantilevers can be excited by external harmonic forces. This can be applied directly to the cantilever, or can be applied by exciting root of the cantilever. Here the formulations are developed for direct excitations only. The ideas presented however can be easily extended to the case of root excitation. When steady-state responses due to harmonic or broadband random excitations are considered, the frequency-domain methods provide most physically intuitive and analytically simplest solutions. Assuming the amplitude of the harmonic excitation as F, from the Laplace transform expression in Eq. (38), the response in the frequency domain can be expressed by substituting $s = \mathrm{i}\omega$ as

$$\left(-\omega^2(1+\Delta) + \mathrm{i}\omega 2\zeta_0\omega_0 + \omega_0^2\right)U_m(\mathrm{i}\omega) = \frac{F}{m_0}. \tag{70}$$

Dividing this by ω_0^2, the frequency response function of the mass-absorbed oscillator can be expressed as

$$U_m(\mathrm{i}\Omega) = \frac{U_{st}}{-\Omega^2(1+\Delta) + 2\mathrm{i}\Omega\zeta_0 + 1}, \tag{71}$$

where the normalised frequency and the static response are given by

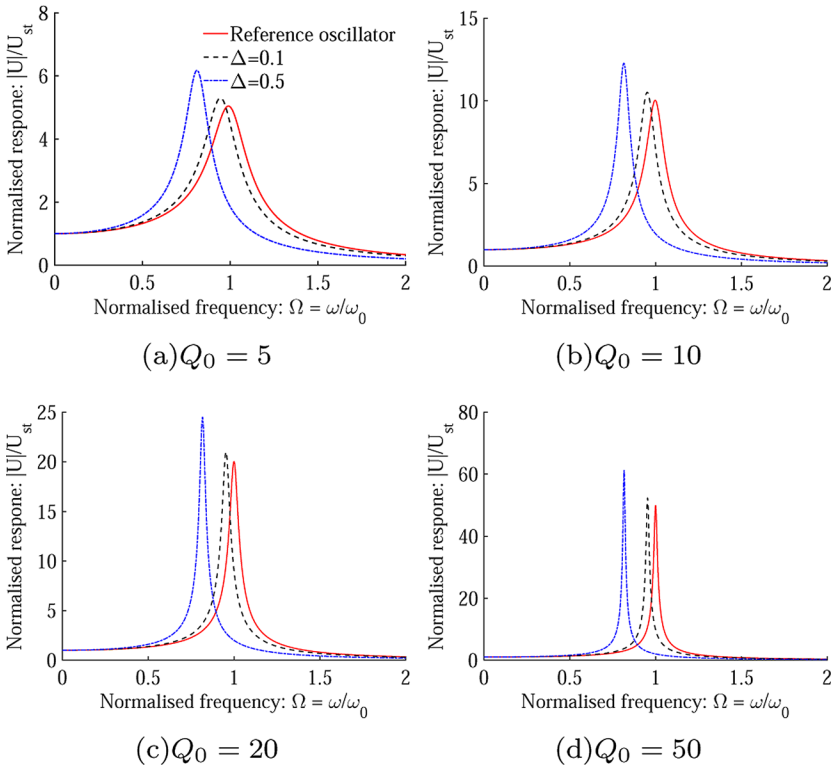

FIG. 6. Normalised response amplitude of the oscillator in the frequency domain as a function of the normalised frequency $\Omega = \omega/\omega_0$ for two different mass absorption factors Δ and four different Q-factors.

$$\Omega = \frac{\omega}{\omega_0} \quad \text{and} \quad U_{st} = \frac{F}{k}. \tag{72}$$

In Fig. 6, the frequency response given by Eq. (71) is plotted by normalising it with U_{st}. It can be observed that the mass-absorbed oscillators show a reduced resonance frequency and reduced damping for all Q-factor values of the reference oscillator. Although the nature of the frequency response changes (sharper for higher Q-factor), the behaviour of frequency and damping shift is consistent to what was observed in Secs. IV A and IV B [see for example Eqs. (41) and (42)]. Next, we propose few strategies to obtain the value of the absorbed mass based on the changes in the frequency response observed in Fig. 6.

1. The peak response method

Frequency response functions such as the ones shown in Fig. 6 can be obtained by the Fast Fourier Transform (FFT) of a measured readout signal in the time domain. In practice, the natural frequency and the damping factor are often obtained from the frequency response function measurements. Therefore, the natural frequency and the damping factor are effectively obtained by "post-processing" the frequency response functions. In some cases, this process can introduce errors. Here we develop a mass sensing approach that directly uses the frequency response function and avoids direct derivation of the natural frequency and the damping factor.

We assume that the maxima or the peak of the frequency response function can be located and measured. In Fig. 7 the peak of the frequency response of the reference oscillator and the mass-absorbed oscillator are shown. The shift in frequency, as well as damping, is marked in the plot. The aim is to utilise both of these information *simultaneously* to obtain an estimate of the absorbed mass.

To obtain the maxima of the frequency response, we take square of the amplitude given by Eq. (71) and set its derivative with respect to Ω^2 to zero, that is

$$\frac{d|U_m|^2}{d\Omega^2} = 0$$
$$\text{or} \quad \frac{d}{d\Omega^2}\left\{\frac{1}{(1-\Omega^2(1+\Delta))^2 + 4\Omega^2\zeta_0^2}\right\} = 0. \tag{73}$$

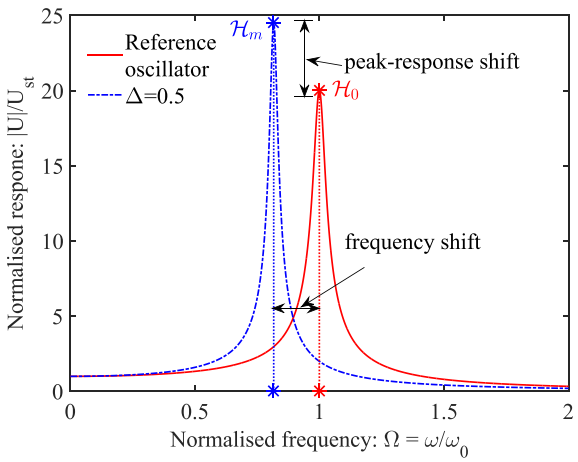

FIG. 7. Normalised response amplitude of the oscillator in the frequency domain as a function of the normalised frequency $\Omega = \omega/\omega_0$ for mass absorption factor $\Delta = 0.5$ and $Q_0 = 20$. $\mathcal{H}_0, \mathcal{H}_m$: Maxima of the frequency response of the reference oscillator and the mass absorbed oscillator.

Solving this equation for Ω, it can be shown that the normalised frequency corresponding to maximum frequency response amplitude is given by

$$\Omega_{\max} = \frac{\sqrt{1+\Delta-2\zeta_0^2}}{1+\Delta} = \sqrt{1-2\zeta_m^2}. \tag{74}$$

The normalised (by U_{st}) amplitude of the maximum response at the above frequency point can be obtained as

$$\mathcal{H}_m = |U_m(\mathrm{i}\Omega = \mathrm{i}\Omega_{\max})|/U_{st} = \frac{1+\Delta}{2\zeta_0\sqrt{1+\Delta-\zeta_0^2}} = \frac{1}{2\zeta_m\sqrt{1-\zeta_m^2}}. \tag{75}$$

In a similar way, the maximum frequency response for the reference oscillator $\mathcal{H}_0$ can also be expressed. Assuming that the maximum frequency response for the reference oscillator and the mass-absorbed oscillator has been experimentally measured, we propose an approach for obtaining the mass absorption factor.

Taking the ratio of the maximum frequency response for both the oscillators we have

$$R_{\mathcal{H}} = \frac{\mathcal{H}_m}{\mathcal{H}_0} = (1+\Delta)\frac{\sqrt{1-\zeta_0^2}}{\sqrt{1+\Delta-\zeta_0^2}}. \tag{76}$$

Squaring both sides, this equation can be simplified to a quadratic equation in Δ. Solving that equation and keeping only the relevant root, the mass absorption factor can be obtained as

$$\Delta = \frac{R_{\mathcal{H}}\left(R_{\mathcal{H}} + \sqrt{R_{\mathcal{H}}^2 - 4\zeta_0^2 + 4\zeta_0^4}\right)}{2\left(1-\zeta_0^2\right)} - 1, \tag{77}$$

$$= (R_{\mathcal{H}}^2 - 1)\left(1 + \zeta_0^2 + \frac{R_{\mathcal{H}}^2+1}{R_{\mathcal{H}}^2}\zeta_0^4 + \cdots\right). \tag{78}$$

The last equation was obtained by a Taylor series expansion of the expression of Δ in Eq. (77) about $\zeta_0 = 0$. For systems with high Q-factor, neglecting higher-order terms in ζ_0, the absorbed mass can be explicitly expressed in terms of the peak responses of both the oscillators as

$$\Delta \approx \left\{\left(\frac{\mathcal{H}_m}{\mathcal{H}_0}\right)^2 - 1\right\}\left(1+\zeta_0^2\right). \tag{79}$$

For further lightly damped systems ($\zeta_0^2 \ll 1$) we have the following simplification:

$$\Delta \approx \left(\frac{\mathcal{H}_m}{\mathcal{H}_0}\right)^2 - 1. \tag{80}$$

Neither the calculation of the resonance frequencies nor the calculation of the damping factors are required to apply this expression. This result is also independent of the Q-factor of the oscillator. Since the frequency response maxima amplitudes appear as a ratio in Eq. (80), units of measurements or normalisation do not affect the result. From the point of view of ease of measurements, Eq. (80) represents the simplest mass sensing approach.

2. The half-power point method

Half-power (frequency) points refer to those frequency values for which the response amplitude square is half of that of the maximum amplitude square. If the response amplitude is considered, this amounts to a reduction of $1/\sqrt{2}$ of the amplitude. If one uses the decibel scale, then this reduction is $20\log_{10}\left(1/\sqrt{2}\right) = -3.0103 \approx -3$ db. The half-power points are often used to obtain the damping factor of an oscillator[48–52] as the reduction of the response is a direct function of damping. It was established before that the damping factor of the mass-absorbed oscillator is different from the reference oscillator. Therefore, this difference would be reflected in the half-power bandwidths of the oscillators. This is the physical basis of this mass sensing approach.

We assume that the half-power points can be located and the bandwidth can be measured. In Fig. 8 the half-power points of the reference oscillator and the mass-absorbed oscillator are shown. The aim is to utilise the difference in the half-power bandwidths to obtain the mass absorption factor Δ. By definition, the half-power points are obtained from the following relationship:

$$|U_m(\mathrm{i}\Omega)|^2 = \frac{\mathcal{H}_m^2}{2}, \tag{81}$$

where $\mathcal{H}_m$ is defined in Eq. (75). Expanding the relevant terms and simplifying, the equation governing the half-power points for the mass-absorbed oscillator can be given by

$$(1+\Delta)^4(\Omega^2)^2 - 2(1+\Delta)^2(1+\Delta-2\zeta_0^2)\Omega^2 + (1+\Delta)^2 + 8\zeta_0^2(1+\Delta-\zeta_0^2) = 0. \tag{82}$$

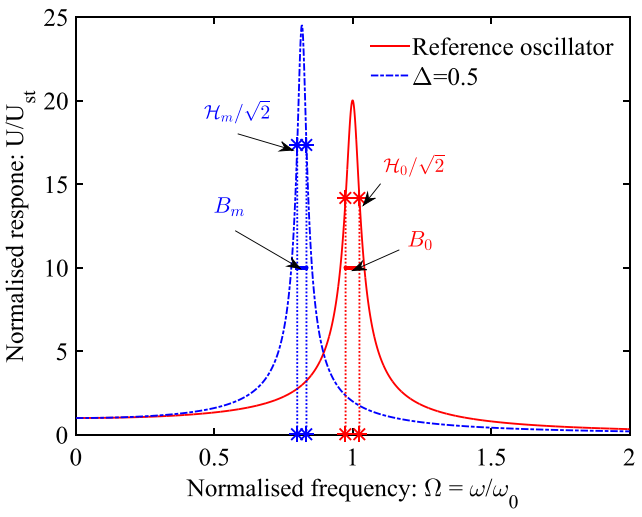

FIG. 8. Half-power points and half-power bandwidths of the reference oscillator (B_0) and the mass-absorbed oscillator (B_m) for $\Delta = 0.5$ and $Q_0 = 20$.

This is a quadratic equation in Ω^2 an can be solved easily to obtain the lower and higher half-power points

$$\Omega_m^{(l,h)} = \frac{\sqrt{(1+\Delta-2\zeta_0^2) \mp 2\zeta_0\sqrt{1+\Delta-\zeta_0^2}}}{1+\Delta}. \tag{83}$$

The half-power bandwidth is defined as the difference between these two points (see Fig. 8) and can be expressed as

$$B_m = \Omega_m^{(h)} - \Omega_m^{(l)}. \tag{84}$$

This quantity can be obtained from experimentally measured frequency response functions. In a similar manner, the half-power bandwidth for the reference oscillator B_0 can also be measured. It is proposed that the shift in the half-power bandwidth to be used for mass sensing. This quantity is expressed as

$$\Delta B = B_0 - B_m = \Omega_0^{(h)} - \Omega_0^{(l)} - (\Omega_m^{(h)} - \Omega_m^{(l)}). \tag{85}$$

Note that in general one expects $B_0 \geq B_m$ as $\zeta_0 \geq \zeta_m$. Using Eqs. (83) and (84), the mass sensing equation in (85) can be expressed as

$$\begin{aligned}\Delta B = &\sqrt{(1-2\zeta_0^2)+2\zeta_0\sqrt{1-\zeta_0^2}} \\ &-\frac{\sqrt{(1+\Delta-2\zeta_0^2)+2\zeta_0\sqrt{1+\Delta-\zeta_0^2}}}{1+\Delta} \\ &-\sqrt{(1-2\zeta_0^2)-2\zeta_0\sqrt{1-\zeta_0^2}} \\ &+\frac{\sqrt{(1+\Delta-2\zeta_0^2)-2\zeta_0\sqrt{1+\Delta-\zeta_0^2}}}{1+\Delta}.\end{aligned} \tag{86}$$

If exact mathematical procedure is followed, it is not possible to obtain the mass absorption factor Δ as a closed-form expression of the half-power bandwidth shift ΔB from this equation. Expanding the right-hand side by a Taylor series about ζ_0, this equation can be simplified after some algebra as

$$\begin{aligned}\Delta B = &2\left(1-\frac{1}{(1+\Delta)}\right)\zeta_0 + 2\left(1-\frac{1}{(1+\Delta)^2}\right)\zeta_0^3 \\ &+7\left(1-\frac{1}{(1+\Delta)^3}\right)\zeta_0^5 + \cdots.\end{aligned} \tag{87}$$

Assuming small damping and therefore ignoring the third and higher order terms in ζ_0, from the above equation, we have

$$\Delta \approx \frac{1}{1-\Delta B/2\zeta_0} - 1 \approx \frac{1}{1-Q_0\Delta B} - 1. \tag{88}$$

This is a simple equation which can be easily applied in practice. Recall that ΔB as defined in (86) is a relative (dimensionless) bandwidth shift. This should be obtained by dividing the actual (dimensional, Hz or rad/s) bandwidth shift with the undamped natural frequency of the reference oscillator.

3. The half-power band area method

The two frequency domain identification techniques suggested before in this section relies on "point estimates." This implies that the value of the identified mass is completely defined by the response measurements at one (for the peak response method) or two (for the half-power point method) frequency points. These approaches are expected to provide accurate results when the measured frequency response functions are free of any noise. However, in many practical situations, some amount of noise in the measured data is inevitable. In such situations, an approach which uses data over many frequency points may be beneficial as the effect of noise may get averaged and in turn, would give more reliable results. This is the motivation behind the approach to be developed in this section. The main idea is that we use the area under the frequency response function within the half-power bandwidth. In this way, the information used in the previous two methods, that is, the peak response and the response at the two half-power points are included along with all the other response points within the band.

The squared-response of the reference oscillator and the mass-absorbed oscillator for $\Delta = 0.5$ and $Q_0 = 10$ are shown in Fig. 9, for example. Unlike the two previous cases, we consider the square of the frequency response function for the ease of the integration. The area within the half-power band width can be obtained as

$$\int_{\Omega(l)}^{\Omega(h)} |U_m|^2 \mathrm{d}\Omega = \int_{\Omega(l)}^{\Omega(h)} \frac{1}{\left(1-\Omega^2(1+\Delta)\right)^2 + 4\Omega^2\zeta_0^2}\mathrm{d}\Omega. \tag{89}$$

Using a transformation of variable $z = \Omega^2$ this integral can be obtained in closed-form as

$$A_m = \frac{\pi}{4\zeta_0\sqrt{1+\Delta-\zeta_0^2}}. \tag{90}$$

From this, we calculate the half-power band area ratio

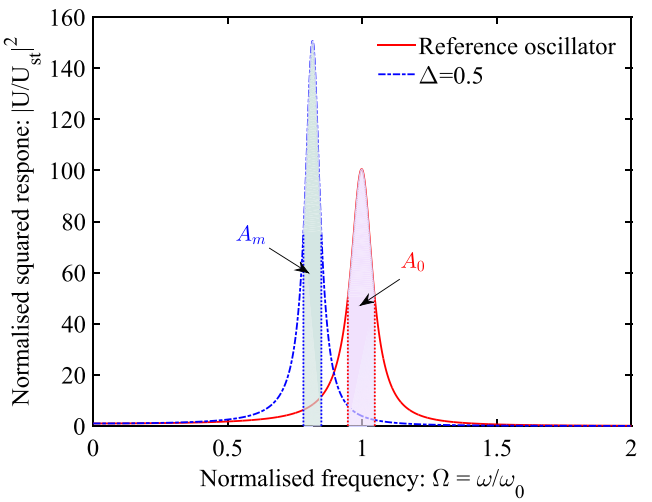

FIG. 9. Squared-response of the reference oscillator and the mass-absorbed oscillator for $\Delta = 0.5$ and $Q_0 = 10$. The shared areas A_m and A_0 represent the area within the half-power bandwidths.

$$\frac{A_0}{A_m} = \frac{\sqrt{1+\Delta-\zeta_0^2}}{\sqrt{1-\zeta_0^2}}. \tag{91}$$

From this relationship, the absorbed mass factor can be expressed as

$$\Delta = (1-\zeta_0^2)\left\{\left(\frac{A_0}{A_m}\right)^2 - 1\right\}. \tag{92}$$

For small damping $\zeta_0^2 \approx 0$ and from Eq. (92), we have the following simplified expression for mass sensing:

$$\Delta \approx \left(\frac{A_0}{A_m}\right)^2 - 1. \tag{93}$$

Therefore, if the area within the half-power band width, as shown in the example in Fig. 9, can be obtained from experimental measurements, Eqs. (92) or (93) can be used for mass sensing.

V. SUMMARY AND CONCLUSIONS

Inertial mass sensing using vibrating microcantilever is discussed. Micromechanical mass sensing exploits a shift in the resonance frequency caused by the absorption of a mass

TABLE I. Summary of mass sensing methods exploiting the damping characteristics of an oscillator. This table lists different closed-form expressions for mass sensing developed in the paper. The undamped natural frequency, damping factor, and Q-factor of the reference oscillator are ω_0, ζ_0, and Q_0.

Methods	Measured quantity	Identified mass absorption factor ($\Delta = \Delta m/m_0$)	Comments
Frequency-shift based methods			
1. Complex frequency shift	s_0, s_m: complex natural frequencies of the reference oscillator and the mass absorbed oscillator, $\Delta\hat{f}^2 = \frac{1}{\omega_0^2}(\lvert s_0\rvert^2 - \lvert s_m\rvert^2)$	$\Delta = \dfrac{1}{1-\Delta\hat{f}^2} - 1$	This is the exact and complete frequency-shift based solution. However, identifying complex frequencies experimentally can be challenging
2. Damped oscillation frequency shift	$\Delta\tilde{f} = \frac{1}{\omega_0}\{\Im(s_0) - \Im(s_m)\}$	$\Delta = -2\Delta\tilde{f}^2 + 4\Delta\tilde{f}\sqrt{1-\zeta_0^2} - 1 + 2\zeta_0^2 + \dfrac{\sqrt{1-4\Delta\tilde{f}^2\zeta_0^2 + 8\Delta\tilde{f}\sqrt{1-\zeta_0^2}\zeta_0^2 - 4\zeta_0^2 + 4\zeta_0^4}}{2\left(-\Delta\tilde{f} + \sqrt{1-\zeta_0^2}\right)^2}$	
3. Oscillation frequency shift	$\Delta\tilde{f}$	$\Delta = \dfrac{1}{(1-\Delta\tilde{f})^2} - 1$	Small damping assumption ($\zeta_0^2 \ll 1, \Im(s_0) \approx \omega_0$)
4. Oscillation frequency shift (approximate)	$\Delta\tilde{f}$	$\Delta \approx 2(\Delta\tilde{f})$	Small damping and also small frequency-shift assumption. This is the *conventional approach* for label-free mass sensing
Methods based on free time-domain response			
5. Logarithmic decrement shift	δ_0, δ_m: Logarithmic decrement of the reference oscillator and the mass absorbed oscillator, and ζ_0	$\Delta = (1-\zeta_0^2)\left\{\left(\dfrac{\delta_0}{\delta_m}\right)^2 - 1\right\}$	Exact and simplest equation. The logarithmic decrement can be measure from the free vibration response in the time domain
6. Logarithmic decrement shift (approximate)	δ_0, δ_m	$\Delta \approx \left(\dfrac{\delta_0}{\delta_m}\right)^2 - 1$	Small damping assumption
Methods based on steady-state frequency-domain response			
7. Peak response shift	$\mathcal{H}_0, \mathcal{H}_m$: Maximum of the frequency response of the reference oscillator and the mass absorbed oscillator, $R_\mathcal{H} = \frac{\mathcal{H}_m}{\mathcal{H}_0}$, and ζ_0	$\Delta = \dfrac{R_\mathcal{H}\left(R_\mathcal{H} + \sqrt{R_\mathcal{H}^2 - 4\zeta_0^2 + 4\zeta_0^4}\right)}{2(1-\zeta_0^2)} - 1$	The maximum points can be obtained graphically from the frequency response plots
8. Peak response shift (approximate)	$\mathcal{H}_0, \mathcal{H}_m, \zeta_0$	$\Delta \approx \left\{\left(\dfrac{\mathcal{H}_m}{\mathcal{H}_0}\right)^2 - 1\right\}(1+\zeta_0^2)$	Small damping such that $\zeta_0^4 \approx 0$.
9. Peak response shift (lightly damped)	$\mathcal{H}_0, \mathcal{H}_m$	$\Delta \approx \left(\dfrac{\mathcal{H}_m}{\mathcal{H}_0}\right)^2 - 1$	Small damping assumption. This is possibly the simplest method to apply in practice
10. Half-power bandwidth shift (approximate)	B_0, B_m: The half-power bandwidth of the reference oscillator and the mass absorbed oscillator, $\Delta B = B_0 - B_m$, and ζ_0 (or Q_0)	$\Delta \approx \dfrac{1}{1-\Delta B/2\zeta_0} - 1 \approx \dfrac{1}{1-Q_0\Delta B} - 1$	Small damping assumption. The half-power bandwidths can be obtained graphically
11. Half-power band area shift	A_0, A_m: Area within the half-power bandwidth of the reference oscillator and the mass absorbed oscillator, and ζ_0	$\Delta = (1-\zeta_0^2)\left\{\left(\dfrac{A_0}{A_m}\right)^2 - 1\right\}$	The areas should be obtained from the (normalised) squared response.
12. Half-power band area shift (approximate)	A_0, A_m	$\Delta \approx \left(\dfrac{A_0}{A_m}\right)^2 - 1$	Small damping assumption

to an existing cantilever. It is suggested that an alternate route to mass sensing is possible by exploiting a "damping factor shift" when the Q-factor of the underlying reference cantilever is low. This approach complements the existing frequency-shift based approach. It is shown that the absorption of a mass to a lightly damped oscillator changes the resonance frequency and the effective damping factor (also the Q-factor) by exactly the same amount. Based on this fundamental observation that the absorption of a mass to an existing cantilever changes its effective damping behaviour, three new approaches to mass sensing are proposed. These methods are based on (a) frequency shifts in the complex plane, (b) damped free vibration response in the time domain, and (c) the steady-state response in the frequency domain. A summary of the methods and their corresponding closed-form expressions for mass sensing is given in Table I. In total, 12 equations are listed which can be used for mass sensing from different damped dynamic measurements. The first group of methods utilise the shift in the (squared) complex natural frequency and damped resonance frequency. Note that conventional frequency measurement techniques usually measure the damped resonance frequency and not the complex natural frequency (as this also contains the decay information). The second group of methods utilise the shift in the logarithmic decrement, which can be measured directly from the free vibration response in the time domain due to some initial conditions (velocity or displacement). The third group of methods utilise the shifts in the maxima of the frequency response function, half-power bandwidth, and the area within the half-power bandwidth.

These new mass sensing expressions can be employed when the frequency shift analysis becomes difficult, as in a low Q-system. They can be applied in conjunction with the conventional frequency shift analysis. Results using these approaches can either be used to validate frequency-shift based results or can be averaged to obtain more robust and consistent results. One can even employ more than one methods proposed here and compare the values of the identified mass and check for consistency.

These analytical expressions broaden the horizon of mass sensing and open up the immense possibility of utilising multiple experimental measurements simultaneously. Future research needs to be directed towards experimental investigations involving the ideas presented here. The experimental techniques for measuring the natural frequencies have evolved over the years to be extremely precise, compared to any other quantities such as the damping factor. The proposed methods should be viewed not only from the point of view of the underlying mathematical methods, but also from the possible sources or experimental errors in the necessary quantities listed in Table I. Future research is necessary for rigorous error analysis and sensitivity with respect to noise in the measured data.

[1]A. Boisen, S. Dohn, S. S. Keller, S. Schmid, and M. Tenje, "Cantilever-like micromechanical sensors," Rep. Prog. Phys. **74**, 036101 (2011).
[2]J. Tamayo, P. M. Kosaka, J. J. Ruz, A. San Paulo, and M. Calleja, "Biosensors based on nanomechanical systems," Chem. Soc. Rev. **42**, 1287–1311 (2013).
[3]K. Ekinci and M. Roukes, "Nanoelectromechanical systems," Rev. Sci. Instrum. **76**, 061101 (2005).
[4]M. Li, H. X. Tang, and M. L. Roukes, "Ultra-sensitive NEMS-based cantilevers for sensing, scanned probe and very high-frequency applications," Nat. Nanotechnol. **2**, 114–120 (2007).
[5]Y. Yang, C. Callegari, X. Feng, K. Ekinci, and M. Roukes, "Zeptogram-scale nanomechanical mass sensing," Nano Lett. **6**, 583–586 (2006).
[6]J. Mertens, C. Rogero, M. Calleja, D. Ramos, J. Angel Martin-Gago, C. Briones, and J. Tamayo, "Label-free detection of DNA hybridization based on hydration-induced tension in nucleic acid films," Nat. Nanotechnol. **3**, 301–307 (2008).
[7]M. Calleja, M. Nordstrom, M. Alvarez, J. Tamayo, L. Lechuga, and A. Boisen, "Highly sensitive polymer-based cantilever-sensors for DNA detection," Ultramicroscopy **105**, 215–222 (2005).
[8]A. Boisen, "Mass spec goes nanomechanical," Nat. Nanotechnol. **4**, 404–405 (2009).
[9]J. L. Arlett, E. B. Myers, and M. L. Roukes, "Comparative advantages of mechanical biosensors," Nat. Nanotechnol. **6**, 203–215 (2011).
[10]M. Alvarez, A. Calle, J. Tamayo, L. Lechuga, A. Abad, and A. Montoya, "Development of nanomechanical biosensors for detection of the pesticide DDT," Biosens. Bioelectron. **18**, 649–653 (2003).
[11]J. Tamayo, A. Humphris, A. Malloy, and M. Miles, "Chemical sensors and biosensors in liquid environment based on microcantilevers with amplified quality factor," Ultramicroscopy **86**, 167–173 (2001).
[12]M. S. Hanay, S. Kelber, A. K. Naik, D. Chi, S. Hentz, E. C. Bullard, E. Colinet, L. Duraffourg, and M. L. Roukes, "Single-protein nanomechanical mass spectrometry in real time," Nat. Nanotechnol. **7**, 602–608 (2012).
[13]M. Calleja, J. Tamayo, M. Nordstrom, and A. Boisen, "Low-noise polymeric nanomechanical biosensors," Appl. Phys. Lett. **88**, 113901 (2006).
[14]J. Mertens, M. Alvarez, and J. Tamayo, "Real-time profile of microcantilevers for sensing applications," Appl. Phys. Lett. **87**, 234102 (2005).
[15]C. Y. Li and T. W. Chou, "Mass detection using carbon nanotube-based nanomechanical resonators," Appl. Phys. Lett. **84**, 5246–5248 (2004).
[16]K. Jensen, K. Kim, and A. Zettl, "An atomic-resolution nanomechanical mass sensor," Nat. Nanotechnol. **3**, 533–537 (2008).
[17]E. Gil-Santos, D. Ramos, A. Jana, M. Calleja, A. Raman, and J. Tamayo, "Mass sensing based on deterministic and stochastic responses of elastically coupled nanocantilevers," Nano Lett. **9**, 4122–4127 (2009).
[18]R. Chowdhury, S. Adhikari, and J. Mitchell, "Vibrating carbon nanotube based bio-sensors," Physica E **42**, 104–109 (2009).
[19]Y. Li, X. Qiu, F. Yang, X.-S. Wang, and Y. Yin, "Ultra-high sensitivity of super carbon-nanotube-based mass and strain sensors," Nanotechnology **19**, 165502 (2008).
[20]B. L. Allen, P. D. Kichambare, and A. Star, "Carbon nanotube field-effect-transistor-based biosensors," Adv. Mater. **19**, 1439–1451 (2007).
[21]R. Chowdhury and S. Adhikari, "Boron nitride nanotubes as zeptogram-scale bio-nano sensors: Theoretical investigations," IEEE Trans. Nanotechnol. **10**, 659–667 (2011).
[22]X. L. Feng, C. J. White, A. Hajimiri, and M. L. Roukes, "A self-sustaining ultrahigh-frequency nanoelectromechanical oscillator," Nat. Nanotechnol. **3**, 342–346 (2008).
[23]S. Adhikari and R. Chowdhury, "Zeptogram sensing from gigahertz vibration: Graphene based nanosensor," Physica E **44**, 1528–1534 (2012).
[24]E. Sage, A. Brenac, T. Alava, R. Morel, C. Dupre, M. S. Hanay, M. L. Roukes, L. Duraffourg, C. Masselon, and S. Hentz, "Neutral particle mass spectrometry with nanomechanical systems," Nat. Commun. **6**, 6482 (2015).
[25]T. Murmu and S. Adhikari, "Nonlocal frequency analysis of nanoscale biosensors," Sens. Actuators, A **173**, 41–48 (2012).
[26]X. C. Zhang, E. B. Myers, J. E. Sader, and M. L. Roukes, "Nanomechanical torsional resonators for frequency-shift infrared thermal sensing," Nano Lett. **13**, 1528–1534 (2013).
[27]Z. Davis and A. Boisen, "Aluminum nanocantilevers for high sensitivity mass sensors," Appl. Phys. Lett. **87**, 013102 (2005).
[28]S. Adhikari and R. Chowdhury, "The calibration of carbon nanotube based bio-nano sensors," J. Appl. Phys. **107**, 124322 (2010).
[29]S. Dohn, W. Svendsen, A. Boisen, and O. Hansen, "Mass and position determination of attached particles on cantilever based mass sensors," Rev. Sci. Instrum. **78**, 103303 (2007).
[30]S. Dohn, S. Schmid, F. Amiot, and A. Boisen, "Position and mass determination of multiple particles using cantilever based mass sensors," Appl. Phys. Lett. **97**, 044103 (2010).

[31]S. Adhikari and T. Murmu, "Nonlocal mass nanosensors based on vibrating monolayer graphene sheets," Sens. Actuators, B **188**, 1319–1327 (2013).
[32]R. Lifshitz and M. Roukes, "Thermoelastic damping in micro- and nanomechanical systems," Phys. Rev. B **61**, 5600–5609 (2000).
[33]K. Y. Yasumura, T. D. Stowe, E. M. Chow, T. Pfafman, T. W. Kenny, B. C. Stipe, and D. Rugar, "Quality factors in micron- and submicron-thick cantilevers," J. Microelectromech. Syst. **9**, 117–125 (2000).
[34]P. Mohanty, D. Harrington, K. Ekinci, Y. Yang, M. Murphy, and M. Roukes, "Intrinsic dissipation in high-frequency micromechanical resonators," Phys. Rev. B **66**, 085416 (2002).
[35]S. Schmid and C. Hierold, "Damping mechanisms of single-clamped and prestressed double-clamped resonant polymer microbeams," J. Appl. Phys. **104**, 093516 (2008).
[36]F. R. Blom, S. Bouwstra, M. Elwenspoek, and J. H. J. Fluitman, "Dependence of the quality factor of micromachined silicon beam resonators on pressure and geometry," J. Vac. Sci. Technol. B: Microelectron. Nanometer Struct. Process., Meas., Phenom. **10**, 19–26 (1992).
[37]J. E. Sader, "Frequency response of cantilever beams immersed in viscous fluids with applications to the atomic force microscope," J. Appl. Phys. **84**, 64–76 (1998).
[38]C. A. V. Eysden and J. E. Sader, "Frequency response of cantilever beams immersed in viscous fluids with applications to the atomic force microscope: Arbitrary mode order," J. Appl. Phys. **101**, 044908 (2007).
[39]B. J. Lazan, *Damping of Materials and Members in Structural Mechanics* (Pergamon Press, Oxford, 1968).
[40]C. Beards, *Structural Vibration: Analysis and Damping* (ButterHeinem ST, Oxford, UK, 1996).
[41]S. Adhikari, *Structural Dynamic Analysis with Generalized Damping Models: Analysis* (Wiley ISTE, UK, 2013).
[42]S. Adhikari, *Structural Dynamic Analysis with Generalized Damping Models: Identification* (Wiley ISTE, UK, 2013).
[43]H. T. Banks and D. J. Inman, "On damping mechanisms in beams," Trans. ASME - J. Appl. Mech. **58**, 716–723 (1991).
[44]R. D. Blevins, *Formulas for Natural Frequency and Mode Shape* (Krieger Publishing Company, Malabar, FL, USA, 1984).
[45]L. Meirovitch, *Principles and Techniques of Vibrations* (Prentice-Hall International, Inc., New Jersey, 1997).
[46]S. Dohn, R. Sandberg, W. Svendsen, and A. Boisen, "Enhanced functionality of cantilever based mass sensors using higher modes," Appl. Phys. Lett. **86**, 233501 (2005).
[47]D. J. Inman, *Engineering Vibration* (Prentice Hall PTR, NJ, USA, 2003).
[48]H. Yin, "A new theoretical basis for the bandwidth method and optimal power ratios for the damping estimation," Mech. Syst. Signal Process. **22**, 1869–1881 (2008).
[49]J.-T. Wang, F. Jin, and C.-H. Zhang, "Estimation error of the half-power bandwidth method in identifying damping for multi-dof systems," Soil Dyn. Earthquake Eng. **39**, 138–142 (2012).
[50]G. A. Papagiannopoulos and G. D. Hatzigeorgiou, "On the use of the half-power bandwidth method to estimate damping in building structures," Soil Dyn. Earthquake Eng. **31**, 1075–1079 (2011).
[51]B. Wu, "A correction of the half-power bandwidth method for estimating damping," Arch. Appl. Mech. **85**, 315–320 (2015).
[52]J. Wang, D. Lü, F. Jin, and C. Zhang, "Accuracy of the half-power bandwidth method with a third-order correction for estimating damping in multi-dof systems," Earthquake Eng. Eng. Vib. **12**, 33–38 (2013).